COVID-19 Diagnosis Using Deep Learning

Gür Emre GÜRAKSIN [a], Sezin BARIN [b,*], Esra ÖZGÜL [c], Furkan KAYA [c]

[a] *Computer Engineering Department, Engineering Faculty, Afyon Kocatepe University, Afyonkarahisar, TURKEY*

[b] *Biomedical Engineering Department, Engineering Faculty, Afyon Kocatepe University, Afyonkarahisar, TURKEY*

[c] *Radiology Department, Faculty of Medicine, Afyonkarahisar Health Sciences University, Afyonkarahisar, TURKEY*

* *Corresponding Author's email address: sbarin@aku.edu.tr*
DOI: 10.29130/dubited.866124

ABSTRACT

The coronavirus, which appeared in Wuhan city of China and named COVID-19 , spread rapidly and caused the death of many people. Early diagnosis is very important to prevent or slow the spread. The first preferred method by clinicians is real-time reverse transcription-polymerase chain reaction (RT-PCR). However, expected accuracy values cannot be obtained in the diagnosis of patients in the incubation period. Therefore, common lung devastation in COVID-19 patients were considered and radiological lung images were used to diagnose. In this study, automatic COVID-19 diagnosis was made from posteroanterior (PA) chest X-Ray images by deep learning method. In the study, using two different deep learning methods, classification was made with different dataset combinations consisting of healthy, COVID, bacterial pneumonia and viral pneumonia X-ray images. The results show that the proposed deep learning-based system can be used in the clinical setting as a supplement to RT-PCR test for early diagnosis

Anahtar Kelimeler: Deep Learning, COVID-19, GoogleNet, AlexNet, X-ray Imaging

Derin Öğrenme Yöntemleri ile COVID-19 Teşhisi

ÖZET

Çin'in Wuhan şehrinde ortaya çıkan ve COVID-19 olarak adlandırılan koronovirüsü dünyanın çok büyük bir kısmını etkisi altına alarak hızla yayılmış ve birçok insanın ölümüne yol açmıştır. Yayılmanın önlenmesi veya yavaşlatılması için erken teşhis oldukça önemlidir. Klinisyenler tarafından ilk tercih edilen yöntem gerçek zamanlı ters transkripsiyon-polimeraz zincir reaksiyonu (RT-PCR) olmaktadır. Ancak kuluçka dönemindeki hastaların teşhisinde beklenen doğruluk değerleri elde edilememektedir. Bu nedenle COVID-19 hastalarında ortak olarak görülen akciğer hasarları göz önüne alınmış ve radyolojik akciğer görüntüleri teşhis koymak için kullanılmıştır. Bu çalışmada posteroanterior(PA) göğüs X-Ray görüntülerinden derin öğrenme yöntemi ile otomatik COVID-19 teşhisi yapılmıştır. Çalışmada iki farklı derin öğrenme yöntemi kullanılarak, sağlıklı,covid,bacterial pneumonia ve viral pneumonia X-ray görüntüleri bulunan sınıflardan oluşan farklı veriseti kombinasyonları ile sınıflandırma yapılmıştır. Elde edilen sonuçlar önerilen derin öğrenme tabanlı sistemin erken teşhis için RT-PCR testini destekleyici olarak klinik ortamda kullanılabileceğini göstermektedir.

Keywords: Derin Öğrenme, COVID-19, GoogleNet, AlexNet, X-ray Görüntüleme

I. INTRODUCTION

Coronavirus belongs to a large family of viruses that cause disease in animals or humans [1]. Many different types of coronaviruses have occurred in humans that cause either colds or severe respiratory infections, including Middle East Respiratory Syndrome (MERS) and Severe Acute Respiratory Syndrome (SARS). On December 31, 2019, a pneumonia diagnosis with an unknown cause was identified in Wuhan, China, and subsequently reported to the World Health Organization (WHO). As a result of the analyzes, the presence of a new type of coronavirus was detected [1]–[4]. This virus, called COVID-19 by WHO on February 11, 2020, has rapidly spread worldwide in a short time and caused many deaths, such that a Public Health Emergency of International Concern was announced on January 30, 2020 [1], [3], [4]. The known mild symptoms of COVID-19 are fever, fatigue, dry cough, pain, nasal congestion, runny nose, sore throat, and diarrhea. However, 1 out of 6 people reportedly has high fever, intense cough, difficulty breathing, and require medical assistance[1]–[4]. Decreasing the spreading rate of COVID-19, which currently has no cure, is the most basic measure that can be taken until an acceptable treatment method becomes available. Early diagnosis is crucial in reducing the rate of spread. However, RT-PCR method, which is the first choice in diagnosing the disease, does not show the expected performance in diagnosing patients who are in the incubation period[5], [6]. This has prompted researchers to look for different methods for early diagnosis.

In a study published by Huang et al.[7] , the clinical findings of 41 patients diagnosed with COVID-19 and hospitalized in Wuhan until January 2, 2020 were reported. In the article, all patients were reported to have pneumonia with abnormal findings in their thorax CT. In another study conducted by Song et al.[8], in the thorax CT of 51 patients, pure ground-glass opacities (GGO) were present in 77% of the patients, GGOs with interstitial and/or interlobular septal thickening in was visible in 75% of the patients, whereas 59% of the patients had GGOs with consolidation. Xie et al.[6] used 167 patient data in their study. While 5 (3%) of these patients had negative RT-PCR in the beginning, a positive thorax CT with a pattern compatible with viral pneumonia was identified. Similarly, while the RT-PCR test was positive for seven patients (4%), their CT diagnosis was initially negative. For the remaining 155 patients (93%), both RT-PCR and CT were positive for COVID-19. These results have increased the importance of studies on thorax CT and chest x-ray images for early diagnosis and diagnosis of COVID-19.

Deep learning has recently become the first-choice method for medical image processing due to its high success rate. This is a widely used method for several tasks with an increasingly high medical diagnosis application due to the successful classification and segmentation of medical images. There has been a surge in studies involving deep learning methods for the classification of CT and X-ray images for the diagnosis of COVID-19 in the literature. Abbas et al. [9] collated data from two sources: 105 COVID-19, and 11 SARS chest x-ray images from the dataset created by Cohen et al.[10] and 80 normal chest x-ray images taken from the Japanese Society of Radiological Technology (JSRT). Due to the low number of images in the dataset, the authors employed data augmentation operations, including up/down and right/left flipping, translation, and rotation methods from 5 different angles, to obtain a total of 1764 images. The Convolutional Neural Network (CNN) based transfer learning method with Decompose Transfer and Compose (DeTraC) was used to classify the images in their dataset. ResNet-18 was preferred at the Transfer stage of the DeTraC method. In a study conducted by Wang et al. [11], the Chest X-Ray Images (Pneumonia)[12] available on the Kaggle public dataset site was selected for binary classification. This data set comprised 4273 pneumonia and 1583 normal images. In order to resolve the data imbalance, various data augmentation methods including rescaling, rotations, shifts, zooms and flips were applied. CNN-based transfer learning methods including VGG16, VGG19, DenseNet201, Inception_ResNet_V2, Inception_V3, Resnet50, MobileNet_V2, and Xception deep learning architectures were selected for the classification task. The authors reported that the Resnet50, MobileNet_V2, and Inception_Resnet_V2 architectures gave more successful results. The remarkable aspect of this study is the fact that no original COVID-19 images were used. The study was based on the diagnosis of pneumonia in chest X-ray images of patients diagnosed with COVID-19. In a study conducted by Alqudah et al.[5], the authors selected the publicly available ieee8023/covid-chestxray-

dataset[10] (which was created using Chest X-Ray Images (Pneumonia)[12]). They employed data augmentation techniques to produce the Augmented COVID-19 X-ray Images Dataset [13], which they employed for their studies. In their study, the authors carried out binary classification of COVID-19 and No-COVID-19 using Support Vector Machine (SVM), Random Forest (RF), and Convolutional Neural Network (CNN). In another study by Xu et al.[14], 219 COVID-19, 224 Influenza-A, and 175 normal 618 CT images were used for classification experiments. The study consisted of image preprocessing, segmentation, and classification stages. The VNET-based VNET-IR-RPN segmentation model was used for segmentation. For classification experiments, they selected the CNN-based ResNet-18 model and created other CNN models based on the architecture of the ResNet-18 model. The study by Chowdhury et al.[15] employed a dataset that was created by combining four different data sets[10], [12], [16], [17]. They applied data augmentation techniques, including rotation, scaling, and translation. They investigated binary classification (Normal/COVID-19) and multi-classification (Normal / COVID-19 / Viral Pneumonia) problems using AlexNet, ResNet18, DenseNet201 and SqueezeNet deep learning architectures. Hemdan et al.[18] investigated binary classification using 25 normal and 25 COVID-19 chest X-ray images taken from the public dataset [10]. They employed transfer learning models including VGG19, DenseNet201, InceptionV3, ResNetV2, InceptionResNetV2, Xception, and MobileNetV2 deep neural network architectures. Ghoshal and Tucker[19] studied multi-classification for normal/COVID-19/viral pneumonia/bacterial pneumonia using images obtained from two public databases[10], [12]. Since COVID-19 images were less than other images, the authors applied data augmentation to these images and carried out classification experiments using ResNet50V2 deep neural network architecture. Narin et al.[20] explored binary classification with ResNet50, InceptionV3 and InceptionResNetV2 architectures using 50 COVID-19 and 50 normal images from data sets[10], [12]. Nigam et al.[21] created a dataset of 16634 CT images in total, consisting of 6000 normal, 5634 COVID, and 5000 other viral infections or diseases from hospitals in the Maharashtra and Indore regions of India. In their classification studies using VGG16, DenseNet121, Xception, NASNet, and EfficientNet deep learning architectures achieved an accuracy of 79.01%, 89.96%, 88.03%, 85.03%, and 93.48%, respectively. Serte and Demirel[22] proposed a ResNet-50-based deep learning architecture to diagnose COVID-19 from 3D-CT images. They created a binary classification study using the Mosmed-1110 data set, which obtained 96% AUC, 84% accuracy, 100% sensitivity, and 80% specificity. As mentioned above, the literature's main deficiency is the absence of a sufficiently labeled COVID-19 image dataset.

In this study, which was carried out using two different deep learning methods, posteroanterior (PA) chest X-ray images in 2 public data sets[10], [12] were combined. Thus, 500 normal, 500 bacteria pneumonia and 500 viral pneumonia images from[12] and 160 COVID-19 PA chest X-ray images from[10] were combined into a dataset. Next, the images in the created dataset were pre-examined by two radiologists. GoogleNet and AlexNet deep learning methods were used to classify these data sets. The details of the study and obtained results are reported in the subsequent sections.

The outline of this paper is as follows. In Section II, The details of the data set used are explained. The preprocesses applied to the images are presented, and the deep learning architectures and training parameters involved in the study are mentioned. In Section III, the studies' results are given, the results obtained are interpreted and compared with other studies in the literature. Finally, the work is briefly summarized in chapter 4, Conclusion.

II. METHOD

The study aims to diagnose COVID-19 using the transfer learning method for high accuracy. For this purpose, AlexNet and GoogleNet architectures, which are among the most common using deep learning architectures, were preferred. For the training and testing, images taken from 2 different open source datasets were combined to create a dataset consisting of 1670 chest X-Ray images. Details are explained in the following of the study.

A. DATASET

The dataset used in the study contains 160 COVID-19, 500 normal, 500 bacteria pneumonia, 500 viral pneumonia, thus a total of 1670 chest X-ray images. The 160 COVID-19 images were taken from Cohen et. al.[10] and comprised posteroanterior (PA) chest X-ray and CT images of patients with acute respiratory distress syndrome (ARDS), COVID-19, and MERS were taken from the open-source GitHub site. The 500 normal, 500 bacteria pneumonia and 500 viral pneumonia images were taken from the "Chest X-Ray Images (Pneumonia)"[12] dataset on the open-source Kaggle site. This primary database comprised 1583 normal, 2786 bacterial pneumonia, and 1504 viral pneumonia chest X-ray images. In order to avoid too much imbalance in the study dataset, 500 images were taken from each class. A sample image for each category in the dataset is shown in Figure 1. The created datasets were pre-examined by two radiologists. Figure 3 presents how different classification problems that were investigated using the created dataset.

A 10-fold cross-validation experiment was implemented in this study; thus 10% of the data is used for testing, whereas the remaining 90% for training the model.
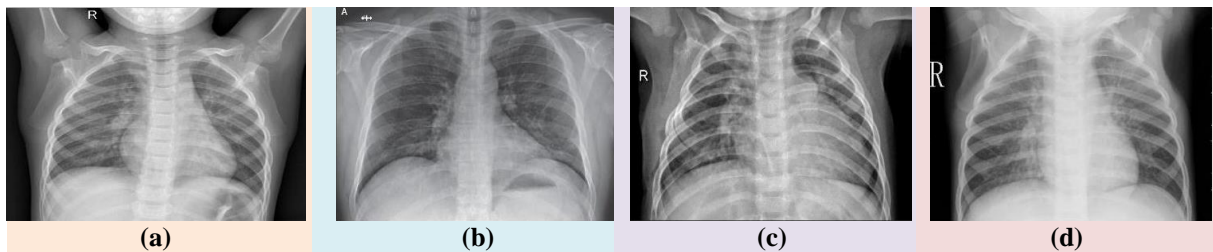

(a)	**(b)**	**(c)**	**(d)**

Figure 1. Sample images for each class in the dataset (a) Healthy, (b) COVID-19, (c) Bacterial Pneumonia, (d) Viral Pneumınia [10], [12]

B. IMAGE PREPROCESSING

The images used in the study were resized in accordance with the requirements of the input layer of the deep convolutional neural network architecture selected for transfer learning application. Accordingly, the images were resized into 224x224x3 and 227x227x3 for the GoogleNet[23] and AlexNet[24] architectures, respectively.

C. APPLICATION OF DEEP LEARNING METHOD

Deep learning, a sub-branch of machine learning inspired by the brain's hierarchical structure, has become an active research area in the literature. Deep artificial neural network architectures contain multi-layers and even layers within layers. They have been effectively employed in image processing methods and eliminates the need for restrictive feature extraction methods. The emergence of advanced computer hardware has also permitted this method to achieve high success and implementations in wide application areas. Deep learning methods, which have seen an increased application in the medical field due to their high achievements, have recently been employed in many areas such as lesion detection, segmentation, and classification of medical images. Figure 2. demonstrates the increasing popularity of deep learning methods in the medical field over the past ten years. This rapid increase can easily be associated with their higher success rates in disease diagnosis and the advancement in the latest technological methods that offer time- and cost-savings [25].
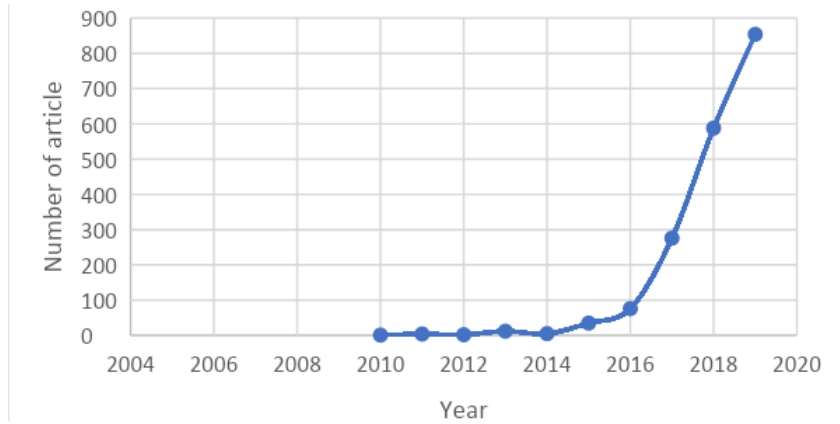
Figure 2. *Number of studies employed for medical imaging publications using deep learning method within the last 10 years* [25]

In this study, 2 CNN-based deep neural network models, trained with ImageNet[26], and purposely developed for object classification and detection, were used. These deep CNN architectures were used to diagnose patients with COVID-19 using the transfer learning method. A transfer learning method provides faster training time and better performance than CNN architectures trained from scratch. The preferred 2 deep neural network architectures for transfer learning in the study are AlexNet and GoogleNet.

D. APPLICATION OF TRANSFER LEARNING

Transfer learning is a deep learning technique that uses the earlier acquired knowledge of a neural network trained for a task and applies it to another related task. In this study, two convoluted neural networks which were trained with ImageNet[26], one of the largest image databases, was employed for the identification of chest X-ray images of patients with COVID-19 disease (PA). These conventional neural networks are AlexNet and GoogleNet. These two architectures were used for different classification processes. In the first classification process involving 4 categories, images are classified as either COVID-19, healthy, bacteria pneumonia or viral pneumonia. The second classification task involved a COVID-19 / healthy / pneumonia classification problem. In the third classification process, the images that were first classified as diseased / healthy were subsequently classified as COVID-19 / pneumonia if diseased diagnosis was predicted. If the images classified as diseased / healthy are diseased, they are again classified as COVID-19 / bacterial pneumonia / viral pneumonia. Inspired by the classification of viral pneumonia / COVID-19 / healthy images carried out by Chowdhury et. al.[15], the limits of the study were extended to carry out viral pneumonia / COVID-19 / healthy and bacteria pneumonia / COVID-19 / healthy classification experiments. The applied classification studies can be easily seen with the flow diagrams shown in Figure 3.
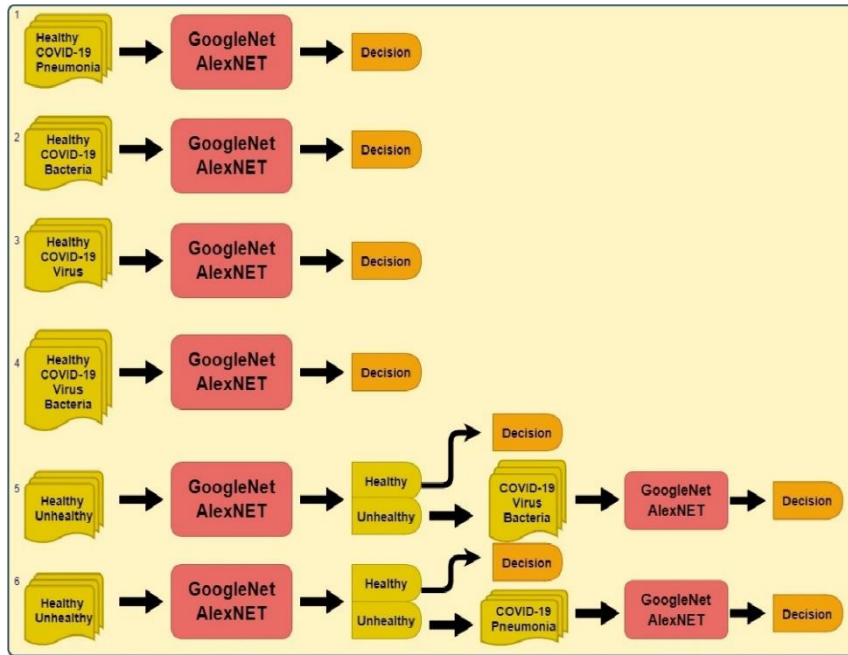
Figure 3. *Flow chart of the study*

D. 1. AlexNet [24]

AlexNet is a CNN architecture designed by Krizhevsky et al.[24]. This model was adjudged the first position in the ImageNet ILSVRC contest in 2012, with 15.3% top-5 best error rate. The 8-layered artificial neural network architecture, which includes three fully connected layers and five convolution layers followed by a maximum pooling layer, ends with the 1000 connected softmax layer. The input layer accepts images with size of 227x227x3. The architecture of the artificial neural network is given in Figure 4.
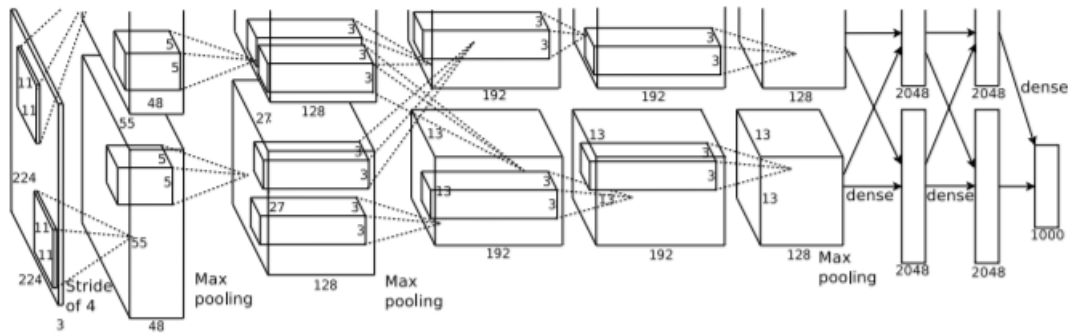
Figure 4. *AlexNet Architecture* [24]

The training parameters of the AlexNet model in the study are the adam optimization function with an initial learning rate of 0.0001, maximum epoch size of 20, and minibatch size of 32.

D. 2. GoogleNet

GoogleNet, also known as Inception-V1[23], is another CNN-based deep learning architecture presented by Szegedy et al.. It was ranked 1st with an error rate of 6.7% in the ImageNet ILSVRC competition held in 2014. Although GoogleNet consists of 22 layers, it reduces the 60 million parameters in AlexNet to 4 million due to the incorporation of an inception module. The input layer accepts images with dimensions 224x224x3. The authors created a network with modules called deep neural network

13

Inception. Each module consists of differently sized convolution and max-pooling layers. The graphical representation of the architecture of GoogleNet is given in Figure 5.

For a fair comparison of the GoogleNet model with the Alex net model, the same training parameters (Adam optimization function with an initial learning rate of 0.0001, maximum epoch size of 20 and minibatch size of 32) were used.
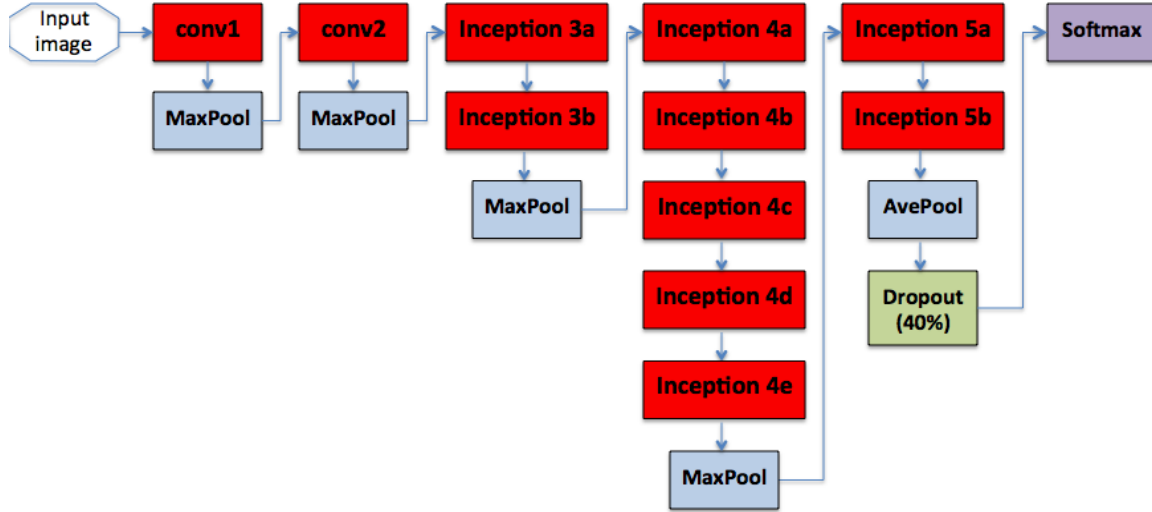
Figure 5. GoogleNet Architecture [23], [27]

The representation of the inception module indicated in Figure 5 can be seen thoroughly in Figure 6. The inception module operates convolutions with different kernel filter sizes simultaneously, providing a solution for the mathematical computation cost and overfitting problem in deep architectures. As can be seen in Figure 6, calculations are made simultaneously in convolution layers with 1x1,3x3 and 5x5 filter sizes in the inception module at the same time. In this way, large-scale and small-scale features in images can be analyzed.
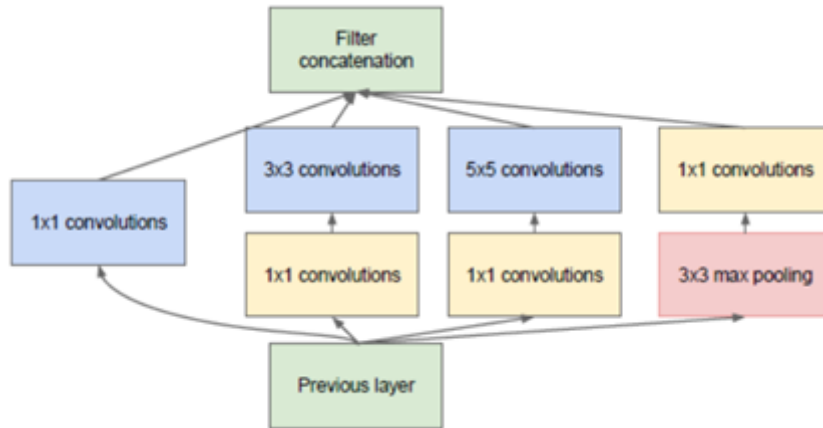
Figure 6. Inception size-reduction module [23]

III. RESULTS AND DISCUSSION

The results of six different experiments (with details presented above), created by combining different classification scenarios, are given in Table 1 for the GoogleNet and AlexNet models. The 10-fold cross-validation method was applied in the study. Therefore, the reported results are the average metrics of the ten folds experiments of each model. Accuracy (mathematical expression in Equation1), Specificity

14

(Equation 2), Sensitivity (Equation 3), and Precision (Equation 4) are the performance evaluation metrics used to measure the success of the study.

$$ACC = \left(\frac{(TP+TN)}{TP+TN+FP+FN}\right) * 100 \tag{1}$$

$$SPEC = \left(\frac{TN}{TN+FP}\right) * 100 \tag{2}$$

$$SENS = \left(\frac{TP}{TP+FN}\right) * 100 \tag{3}$$

$$PREC = \left(\frac{TP}{TP+FP}\right) * 100 \tag{4}$$

The True Positive (TP) value represents the classification of the patient case as a patient, whereas the False Positive (FP) value represents the classification of a healthy case as a patient. The True Negative (TN) value represents the classification of a healthy case as healthy, whereas False Negative (FN) represents the classification of a healthy case as a sick case. Accuracy is the ratio of correctly tagged images relative to all images, whereas Precision represents a situation that assesses whether the image really belongs to the class it was tagged in. Specificity is the correct tagging rate of the images of each class, while the correct tagging rate of the images belonging to the class other than the healthy class is termed sensitivity. The previously mentioned AlexNet and GoogleNet deep learning models were applied to the chest X-ray images created from different classes, and the values obtained from the classification experiments are presented in Table 1. The confusion matrices of the results from the 10-fold cross-validation experiments for AlexNet and GoogleNet are presented in Figures 7 and 8, respectively.

Table 1. *Study results*

		AlexNet	GoogleNet			AlexNet	GoogleNet
Normal Pneumonia COVID-19	**Accuracy**	98.54	<u>98.83</u>	**COVID-19 Virus Bacteria**	**Accuracy**	87.74	<u>89.06</u>
	Sensitivitiy	99.24	99.36				
	Specifity	99.10	99.49		**Sensitivitiy**	92.23	94.08
	Precision	98.04	98.73				
Normal COVID-19 Bacteria	**Accuracy**	<u>98.77</u>	98.59	**Healthy Unhealthy**	**Specifity**	94.38	94.39
	Sensitivitiy	98.88	98.68				
	Specifity	99.76	99.76				
	Precision	99.69	99.47		**Precision**	91.49	92.46
Normal COVID-19 Virus	**Accuracy**	97.56	<u>97.80</u>	**COVID-19 Pneumonia**	**Accuracy**	98.06	<u>98.41</u>
	Sensitivitiy	99.04	99.73				
	Specifity	98.48	98.32				
	Precision	97.24	97.42		**Sensitivitiy**	97.46	96.85
Normal COVID-19 Virus	**Accuracy**	<u>91.38</u>	90.0	**Healthy Unhealthy**	**Sensitivitiy**	93.49	89.56
	Sensitivitiy	93.49	89.56		**Specifity**	98.27	99.23
	Specifity	97.03	97.9				
	Precision	93.32	94.37		**Precision**	96.30	96.66

15

When the data given in Table 1 are examined, all classification evaluations except the accuracy values of the 5th model are over 90%. It shows that the used deep learning architectures can distinguish CT images of COVID-19 patients from healthy and pneumonia patients with an essential accuracy of 98.83%. Also, the height of the sensitivity value indicates that the images belonging to each class are labeled with an accuracy of 99.36%. The specificity value indicates that the images belonging to each class are not labeled with another class label with an accuracy of 99.49%. While the CT images of COVID-19, bacterial pneumonia, and healthy individuals can be classified with an accuracy value of 98.77%, a value loss of 0.93% was observed in CT images' classification of healthy, COVID-19 and, viral pneumonia individuals. There is a serious decrease in the performance of model number 4. This situation shows that the separation of Bacteria and Virus pneumonia images decreases the success. On the other hand, systems numbers 5 and 6, realized in 2 parts, did not show the expected success.

a

Output	Cov.	Norm.	Pneu.	
Cov.	158	0	3	98.1%
Norm.	1	498	7	98.4%
Pneu.	1	2	490	99.4%
	98.8%	99.6%	98.0%	98.8%
	Cov.	Norm.	Pneu.	

Target

b

Output	Bact.	Cov.	Norm.	
Bact.	489	0	3	99.4%
Cov.	0	160	0	100%
Norm.	11	0	497	97.8%
	97.8%	100%	99.4%	98.8%
	Bact.	Cov.	Norm.	

Target

c

Output	Cov.	Norm.	Vir.	
Cov.	158	0	3	98.1%
Norm.	0	496	18	96.5%
Vir.	2	4	479	98.8%
	98.8%	99.2%	95.8%	97.7%
	Cov.	Norm.	Vir.	

Target

e

Output	Norm.	Patie.	
Norm.	492	17	96.7%
Patie.	8	1143	99.3%
	98.4%	98.5%	98.5%
	Norm.	Patie.	

Target

f

Output	Cov.	Pneu.	
Cov.	156	4	97.5%
Pneu.	4	496	99.2%
	97.5%	99.2%	98.8%
	Cov.	Pneu.	

Target

g

Output	Bact.	Cov.	Vir.	
Bact.	444	0	83	84.3%
Cov.	0	157	3	98.1%
Vir.	56	3	414	87.5%
	88.8%	98.1%	82.8%	87.5%
	Bact.	Cov.	Vir.	

Target

d

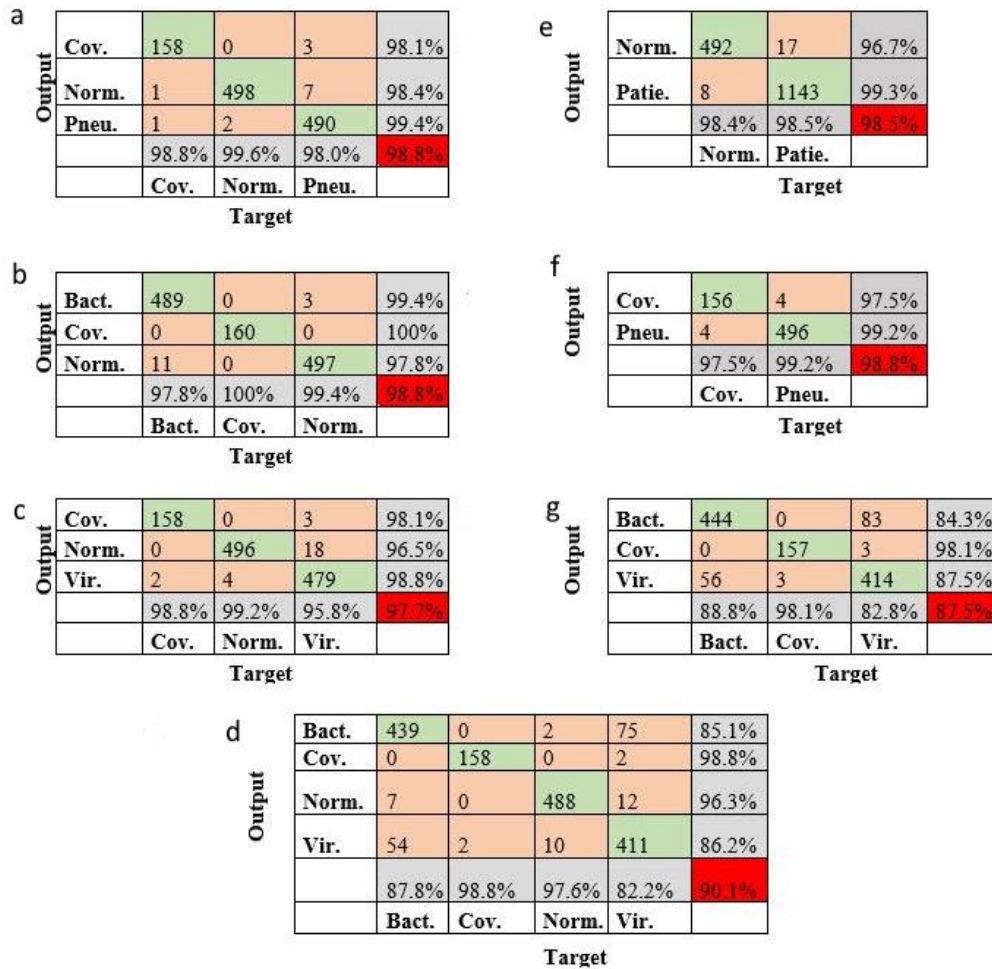| Output	Bact.	Cov.	Norm.	Vir.	
Bact.	439	0	2	75	85.1%
Cov.	0	158	0	2	98.8%
Norm.	7	0	488	12	96.3%
Vir.	54	2	10	411	86.2%
	87.8%	98.8%	97.6%	82.2%	90.1%
	Bact.	Cov.	Norm.	Vir.	

Target

Figure 7. The confusion matrices from the 10-Fold cross-validation experiments of AlexNet; (a) COVID-19, Normal, Pneumonia, (b) COVID-19, Normal, Bacteria, (c) COVID-19, Normal, Virus, (d) COVID-19, Normal, Virus, Bacteria, (e) Normal, Patient, (f) COVID-19, Pneumonia, (g) COVID-19, Virus, Bacteria,
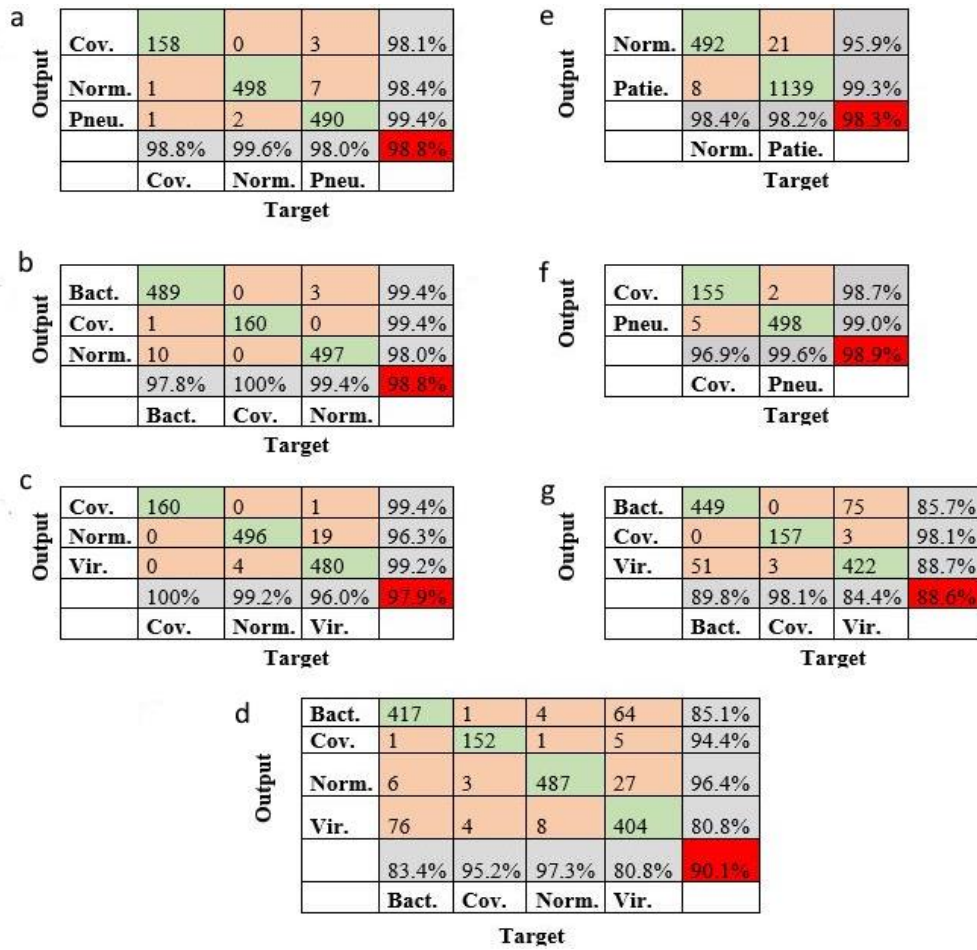
a — COVID-19, Normal, Pneumonia

Output	Cov.	Norm.	Pneu.	
Cov.	158	0	3	98.1%
Norm.	1	498	7	98.4%
Pneu.	1	2	490	99.4%
	98.8%	99.6%	98.0%	98.8%
	Cov.	Norm.	Pneu.	

Target

e — Normal, Patient

Output	Norm.	Patie.	
Norm.	492	21	95.9%
Patie.	8	1139	99.3%
	98.4%	98.2%	98.3%
	Norm.	Patie.	

Target

b — COVID-19, Normal, Bacteria

Output	Bact.	Cov.	Norm.	
Bact.	489	0	3	99.4%
Cov.	1	160	0	99.4%
Norm.	10	0	497	98.0%
	97.8%	100%	99.4%	98.8%
	Bact.	Cov.	Norm.	

Target

f — COVID-19, Pneumonia

Output	Cov.	Pneu.	
Cov.	155	2	98.7%
Pneu.	5	498	99.0%
	96.9%	99.6%	98.9%
	Cov.	Pneu.	

Target

c — COVID-19, Normal, Virus

Output	Cov.	Norm.	Vir.	
Cov.	160	0	1	99.4%
Norm.	0	496	19	96.3%
Vir.	0	4	480	99.2%
	100%	99.2%	96.0%	97.9%
	Cov.	Norm.	Vir.	

Target

g — COVID-19, Virus, Bacteria

Output	Bact.	Cov.	Vir.	
Bact.	449	0	75	85.7%
Cov.	0	157	3	98.1%
Vir.	51	3	422	88.7%
	89.8%	98.1%	84.4%	88.6%
	Bact.	Cov.	Vir.	

Target

d — COVID-19, Normal, Virus, Bacteria

Output	Bact.	Cov.	Norm.	Vir.	
Bact.	417	1	4	64	85.1%
Cov.	1	152	1	5	94.4%
Norm.	6	3	487	27	96.4%
Vir.	76	4	8	404	80.8%
	83.4%	95.2%	97.3%	80.8%	90.1%
	Bact.	Cov.	Norm.	Vir.	

Target

Figure 8. The confusion matrices from the 10-Fold cross-validation experiments of GoogleNet; (a) COVID-19, Normal, Pneumonia, (b) COVID-19, Normal, Bacteria, (c) COVID-19, Normal, Virus, (d) COVID-19, Normal, Virus, Bacteria, (e) Normal, Patient, (f) COVID-19, Pneumonia, (g) COVID-19, Virus, Bacteria,

Considering the results of the study, the cases of pneumonia, COVID-19, and healthy patients are predicted with a high success of 98.83%. However, when the viral pneumonia images are separated, and a subsequent classification carried out, there is a 1.03% decrease in success rate. This can be attributed to the similar features between COVID-19 and viral pneumonia patients. An increase in the number of classification tasks to 4 classes leads to a success rate of 90% as the image similarities increased. However, an examination of the confusion matrices of the four classes in Figures 7 and 8 shows a decrease in the success rate of healthy subjects and a high successful classification of patients with COVID-19 is due to the classification inaccuracies of the viral and bacterial images. The high classification performance of Covid19 / Pneumonia / Healthy images confirms this observation.

As mentioned earlier, the study consisted of two main classification objectives. In this stage, the expected performance could not be achieved as a low classification performance was recorded. The X-ray images of 1160 patients versus 500 healthy X-ray images created an imbalance in the dataset and subsequently affected the first stage of the classification experiments. This issue could be resolved using data augmentation methods, as implemented in other studies in the literature. But this current study did not make such implementations to ensure a fair comparison with classification experiments in the earlier stage.

It is possible to increase the performance of the architectures. The selection of images from different datasets and different hospitals significantly affects the performance of the developed system. But the diversity in the dataset allows wider usability of the developed system. Additionally, increasing the size of the data set can lead to an increase in performance and produce more successful results.

Table 2. *Literature studies and results*

References	Dataset	Method	Output Size	Evaluation Metrics					
				Accuracy	**Sensitivity**	**Specificity**	**Precision**	**Recall**	**F1 Score**
Abbas et. al.[9]	• COVID-19 Image Data Collection [10] • JSRT	• eTraC-ResNet-18	• Normal • COVID-19 • SARS	95.12%	97.91%	91.87%	93.36%	-	-
Wang et. al.[11]	• the Chest X-Ray Images (Pneumonia)[12]	• VGG16 • VGG19 • DenseNet201 Inception_ResNet_V2 • Inception_V3 • Resnet50 • MobileNet_V2 Xception	• Normal • Pneumonia	83%	84%	80.5%	-	-	-
Alqudah et. al. [5]	• COVID-19 Image Data Collection[10] • the Chest X-Ray Images (Pneumonia)[12]	• SVM • Random Forest • CNN	• COVID-19 • No-COVID-19	95.2%	93.3%	100%	100%	-	-
Xu et. al.[14]	• Dataset Collected from the First Affiliated Hospital, College of Medicine, Zhejiang University; Wenzhou Central Hospital; and the First People's Hospital of Wenling	• VNET-IR-RPN • ResNet • CNN	• COVID-19 • No-Infected • Influenza-A	86.7%	-	-	81.3%	86.7%	83.9%

Table 2. *(continuation) Literature studies and results*

Chowdhury et. al.[15]	• COVID-19 Image Data Collection[10] • the Chest X-Ray Images (Pneumonia)[12] • SIRM[16] • Novel Corona Virus 2019 Dataset[17]	• AlexNet • ResNet18 • DenseNet201 • SqueezeNet	• Normal • COVID-19	98.3%	96.7%	100%	100%	-	-
			• Normal • COVID-19 • Viral Pneumonia	98.3%	96.7%	99%	100%	-	-
Hemdan et. al.[18]	• COVID-19 Image Data Collection[10]	• VGG19 • DenseNet201 • InceptionV3 • ResNetV2 • InceptionResNetV2 • Xception • MobileNetV2	• COVID-19 • Normal	90%	-	-	83%	100%	91%
Narin et.al.[20]	• COVID-19 Image Data Collection[10] • the Chest X-Ray Images (Pneumonia)[12]	• ResNet50 • InceptionV3 • InceptionResNetV2	• Normal • COVID-19	98%	-	-	100%	96%	98%
Nigam et.al.[21]	• Dataset Collected from Hospitals in the Maharashtra and Indore regions of India[21]	• VGG16 • DenseNet121 • Xception • NASNet • EfficientNet	• Normal • COVID-19 • Other	93.48%			93%	93%	93%
Serte et. Al.[22]	• Mosmed-1110	• ResNet-50 based architecture	• Normal • COVID-19	0.96 AUC 84% accuracy	100%	80%			

Table 2. *(continuation) Literature studies and results*

Proposed Method	• COVID-19 Image Data Collection[10] • the Chest X-Ray Images (Pneumonia)[12]	• AlexNet • GoogleNet	• Normal • COVID-19 • Pneumonia		98.83%	99.36%	99.49%	98.73%	-	-
			• Normal • COVID-19 • Viral Pneumonia		97.80%	99.73%	98.32%	97.42%	-	-
			• Normal • COVID-19 • Bacteria Pneumonia		98.77%	98.88%	99.76%	99.69%	-	-
			• Normal • Patient	• COVID-19 • Pneumonia	98.41%	96.85%	99.23%	96.66%	-	-
			Normal • Patient	⸲ COVID-19 ⸲ Viral Pneumonia ⸲ Bacteria Pneumonia	89.06 %	94.08 %	94.39 %	92.46 %	-	-
			• Normal • COVID-19 • Viral Pneumonia • Bacteria Pneumonia		91.38%	93.49%	97.03%	93.32%	-	-

A comparison of the study with other published works in the literature given in Table 2 confirms the proposed method outperforms existing methods. In the Literature studies shown in Table 2, it is seen that most of them use deep learning architectures and similar datasets. Also, In Table 2, Deeper architectures are used than the architectures we use, except for the work done by Alqudah et al. However, our performance values are the best result with 98.83% accuracy and among the best results with 99.36% sensitivity, 99.49% specificity, 98.73% precision. The simpler architecture we use provides performance gain while reducing the computational cost. Also, several published works investigated the classification of images into two categories: COVID-19 and No-COVID-19. There is only one study that distinguishes COVID -19 from Pneumonia. However, it is crucial to identify whether a patient's medical condition is caused by viral or bacterial infection. For this reason, this study included various different combinations of classification experiments so as to offer a reference study in the literature and contribute to the medical field.

IV. CONCLUSION

COVID-19 is rapidly spreading worldwide and has caused the death of many people. Early diagnosis has an important role in reducing this spreading rate. A new method is needed to support the accuracy of the RT-PCR test to establish a more successful diagnosis of COVID-19 since the RT-PCR test does not show the accuracy required. Thorax CT has high sensitivity in diagnosis, but its disadvantage of high dose ionizing radiation makes it a less preferable solution. PA lung X-ray radiography, which contains much less radiation, should be used in diagnosis and follow-ups due to the necessity of taking radiological images during the follow-up examination of the patients. PA lung X-ray CT shows insufficient traced ground-glass infiltration. Therefore, PA X-ray is a radiological imaging method with low diagnosis rate of viral pneumonia. It is insufficient to diagnose COVID-19 alone without using deep learning methods. Our study showed that the incorporation of deep learning produced a higher accuracy rate of 98%. Therefore, it can be used in the diagnosis and follow-up examination of the disease.

The symptoms common to all chest X-ray images of all COVID-19 patients are well suited for use in this method. Therefore, in this study, a system was designed to distinguish the images of pneumonia diseases, from healthy patients, as well as the diagnosis of COVID-19 using chest X-ray images. In this system, CNN architectures, GoogleNet and AlexNet architectures, previously trained with a large data set such as ImageNet, are used. A higher performance is expected from the GoogleNet architecture, but it did not perform better than the AlexNet architecture, which even produced better classifications in some instances. An examination of the results shows that more than 98% accuracy was obtained in the diagnosis of COVID-19 disease. However, there is a need to make improvement in distinguishing between viral and bacterial pneumonia patients.

The study created a dataset with images from different sources which impedes a highly successful classification experiment. However, these images taken from different sources rather increased the usage area of the system.

In summary, the proposed deep learning method has the potential to easily overcome difficulties in diagnosing COVID-19 patients in the clinical setting when it is used as an emergency diagnostic tool since it records a high success rate. However, there is a need to train a system with a larger data set and dataset from a single source, which will contribute to increased performance. Thus, an important stage will be achieved for the initial early-stage diagnosis problem of COVID-19.

For future studies, We planned to be expanded with the IoT system, as in similar healthcare-studies in the literature[28]–[30]. In this way, while the patients can be diagnosed remotely, the specialists' increasing workload will be reduced due to the increasing COVID-19 cases. Also, thanks to the data collected through the IoT system, it is possible to overcome the previously mentioned data deficiency problem.

V. REFERENCES

[1]   "Q&A on coronaviruses (COVID-19)." [Online]. Available: https://www.who.int/news-room/q-a-detail/q-a-coronaviruses (accessed Apr. 09, 2020).

[2]   J. Guarner, "Three Emerging Coronaviruses in Two Decades," *Am. J. Clin. Pathol.*, vol. 153, no. 4, pp. 420–421, 2020, doi: 10.1093/ajcp/aqaa029.

[3]   N. N. Chathappady House, S. Palissery, and H. Sebastian, "Corona Viruses: A Review on SARS, MERS and COVID-19," *Microbiol. Insights*, vol. 14, pp. 1–8, 2021, doi: 10.1177/11786361211002481.

[4]   J. Xiao, M. Fang, Q. Chen, and B. He, "SARS, MERS and COVID-19 among healthcare workers: A narrative review," *J. Infect. Public Health*, 2020, doi: 10.1016/j.jiph.2020.05.019.

[5]   A. Alqudah, S. Qazan, H. Alquran, and I. Qasmieh, "Covid-2019 detection using x-ray images and artificial intelligence hybrid systems," *Biomed. Signal Image Anal. Proj. Biomed. Signal Image Anal. Mach. Learn. Lab Boca Raton, FL, USA.*, doi: 10.5455/jjee.204-158531224.

[6]   X. Xie, Z. Zhong, W. Zhao, C. Zheng, F. Wang, and J. Liu, "Chest CT for Typical 2019-nCoV Pneumonia: Relationship to Negative RT-PCR Testing," *Radiology*, 2020, doi: 10.1148/radiol.2020200343.

[7]   C. Huang *et al.*, "Clinical features of patients infected with 2019 novel coronavirus in Wuhan, China," *Lancet*, vol. 395, no. 10223, pp. 497–506, 2020, doi: 10.1016/S0140-6736(20)30183-5.

[8]   F. Song *et al.*, "Emerging 2019 Novel Coronavirus (2019-nCoV) Pneumonia," *Radiology*, vol. 295, no. 1, pp. 210–217, 2020, doi: 10.1148/radiol.2020200274.

[9]   A. Abbas, M. M. Abdelsamea, and M. M. Gaber, "Classification of COVID-19 in chest X-ray images using DeTraC deep convolutional neural network," *Appl. Intell.*, vol. 51, no. 2, pp. 854–864, 2021, doi: 10.1007/s10489-020-01829-7.

[10]   J. P. Cohen, P. Morrison, and L. Dao, "COVID-19 Image Data Collection," *arXiv*, Mar. 2020.
[11]   S. Wang *et al.*, "A deep learning algorithm using CT images to screen for Corona virus disease (COVID-19)," *Eur. Radiol.*, pp. 1–9, 2021, doi: 10.1007/s00330-021-07715-1.

[12]   "Chest X-Ray Images (Pneumonia) | Kaggle." [Online]. Available: https://www.kaggle.com/paultimothymooney/chest-xray-pneumonia (Accessed Apr. 12, 2020).

[13]   A. M. Alqudah and S. Qazan, "Augmented COVID-19 X-ray Images Dataset," *Mendeley Data*, vol. 4, 2020, doi: 10.17632/2FXZ4PX6D8.4.

[14]   X. Xu *et al.*, "A Deep Learning System to Screen Novel Coronavirus Disease 2019 Pneumonia," *Engineering*, vol. 6, no. 10, pp. 1122–1129, 2020, doi: 10.1016/j.eng.2020.04.010.

[15]   M. E. H. Chowdhury *et al.*, "Can AI Help in Screening Viral and COVID-19 Pneumonia?," *IEEE Access*, vol. 8, pp. 132665–132676, 2020, doi: 10.1109/ACCESS.2020.3010287.

[16]   "SIRM | Italian Society of Radiology." [Online]. Available: https://www.sirm.org/en/ (Accessed Apr. 12, 2020).

[17]   "Novel Corona Virus 2019 Dataset | Kaggle." [Online]. Available: https://www.kaggle.com/sudalairajkumar/novel-corona-virus-2019-dataset/kernels (accessed Apr. 12,

2020).

[18]   E. E.-D. Hemdan, M. A. Shouman, and M. E. Karar, "COVIDX-Net: A Framework of Deep Learning Classifiers to Diagnose COVID-19 in X-Ray Images," *arXiv*, 2020.

[19]   B. Ghoshal and A. Tucker, "Estimating Uncertainty and Interpretability in Deep Learning for Coronavirus (COVID-19) Detection," *arXiv*, 2020.

[20]   A. Narin, C. Kaya, and Z. Pamuk, "Automatic Detection of Coronavirus Disease (COVID-19) Using X-ray Images and Deep Convolutional Neural Networks," *arXiv*, 2020.

[21]   B. Nigam, A. Nigam, R. Jain, S. Dodia, N. Arora, and A. B, "COVID-19: Automatic Detection from X-ray images by utilizing Deep Learning Methods," *Expert Syst. Appl.*, 2021, doi: 10.1016/j.eswa.2021.114883.

[22]   S. Serte and H. Demirel, "Deep Learning for Diagnosis of COVID-19 using 3D CT Scans," *Comput. Biol. Med.*, 2021, doi: 10.1016/j.compbiomed.2021.104306.

[23]   C. Szegedy *et al.*, "Going Deeper with Convolutions," in *In Proceedings of the IEEE conference on computer vision and pattern recognition*, 2015, pp. 1–9, doi: 10.1109/CVPR.2015.7298594.

[24]   A. Krizhevsky, I. Sutskever, and G. E. Hinton, "ImageNet Classification with Deep Convolutional Neural Networks," *Adv. Neural Inf. Process. Syst.*, vol. 25, pp. 1097–1105, 2012, doi: 10.1145/3065386.

[25]   "Web of Science [v.5.34] - Web of Science Core Collection Results." http://proxy.afyon.deep-knowledge.net/MuseSessionID=0210h3diw/MuseProtocol=http/MuseHost=apps.webofknowledge.com (Accessed Mar. 31, 2020).

[26]   "ImageNet." [Online]. Available: http://www.image-net.org/ (Accessed Mar. 31, 2020).

[27]   P. Pawara, E. Okafor, O. Surinta, L. Schomaker, and M. Wiering, "Comparing Local Descriptors and Bags of Visual Words to Deep Convolutional Neural Networks for Plant Recognition," *Int. Conf. Pattern Recognit. Appl. Methods* , vol. 2, pp. 479–486, 2017, doi: 10.5220/0006196204790486.

[28]   C. M. J. M. Dourado, S. P. P. da Silva, R. V. M. da Nóbrega, A. C. Antonio, P. P. R. Filho, and V. H. C. de Albuquerque, "Deep learning IoT system for online stroke detection in skull computed tomography images," *Comput. Networks*, vol. 152, pp. 25–39, 2019, doi: 10.1016/j.comnet.2019.01.019.

[29]   D. N. Le, V. S. Parvathy, D. Gupta, A. Khanna, J. J. P. C. Rodrigues, and K. Shankar, "IoT enabled depthwise separable convolution neural network with deep support vector machine for COVID-19 diagnosis and classification," *Int. J. Mach. Learn. Cybern.*, pp. 1–14, 2021, doi: 10.1007/s13042-020-01248-7.

[30]   R. M. Sarmento, F. F. X. Vasconcelos, P. P. R. Filho, and V. H. C. de Albuquerque, "An IoT platform for the analysis of brain CT images based on Parzen analysis," *Futur. Gener. Comput. Syst.*, vol. 105, pp. 135–147, 2020, doi: 10.1016/j.future.2019.11.033.